http://dx.doi.org/10.5012/bkcs.2014.35.3.828

Spectroscopic Properties of Quercetin in AOT Reverse Micelles†

Hyoung-Ryun Park, Seo-Eun Im, Jung-Ja Seo, and Ki-Min Bark‡,*

Department of Chemistry and Research Institute of Basic Science, Chonnam National University, Gwangju 500-757, Korea
*‡Department of Chemical Education, and Research Institute of Life Science, Gyeongsang National University, Chinju 660-701, Korea. *E-mail: kiminb@gnu.ac.kr*
Received September 23, 2013, Accepted October 24, 2013

The spectroscopic properties of quercetin (QCT) were studied in the AOT reverse micelle by fluorescence spectroscopy. Because the molecular structure of QCT is completely planar, excited state intramolecular proton transfer (ESIPT) occurs between the –OH at C(5) and carbonyl oxygen *via* intramolecular hydrogen bonding. This ESIPT happens at the S_1 state but not at the S_2 state. Because QCT is a good donor-acceptor-conjugated molecule at the excited state, this molecule can emit strong fluorescence but shows no $S_1 \rightarrow S_o$ emission due to this ESIPT. Since the $S_2 \rightarrow S_1$ internal conversion was very slow due to the small Franck-Condon factors, $S_2 \rightarrow S_o$ fluorescence emission was observed. All of the experimental results indicated that the QCT resided at the bound water interface and that the position of solute did not change significantly in the micelle at various water concentrations.

Key Words : Quercetin, Fluorescence quantum yield, Fluorescence lifetime, AOT reverse micelle, Intramolecular proton transfer

Introduction

Quercetin (3,3',4',5,7-pentahydroxy flavones; QCT), the polyphenolic compound having –OH group at position 5 (C-5), belongs to the large class of plant pigments called flavonoids. Flavonoids are widely distributed in fruits and vegetables, and have been received a great deal of attention due to their many biological properties, *i.e.*, anticarcinogenic, antiatherosclerotic, antimicrobial, and antioxidant properties.[1-6] QCT is remarkable for its properties to mitigate the increase in capillary fragility, to reduce high blood pressure, to protect plants against the direct and indirect influences of UV radiation and to show antioxidant behaviors against a wide range of free radicals.[7-12]

Flavonoids are well known compounds that exhibit characteristic fluorescence properties.[10,13] QCT has been considered to be composed of a special class of nonfluorescent molecules.[10-12] However, a new significant fluorescence emission was discovered in CH_3OH-H_2O and CH_3CN-H_2O mixed solvents.[14] It would be, therefore, very interesting to study the physicochemical properties of QCT in a specific environment, especially *in vivo*, to better understand the mechanism of its strong biological activity. Since a direct *in vivo* study is difficult, many works have used biologically-mimicking systems such as the AOT reverse micelle and hydro-organic mixed solvents.[15-19]

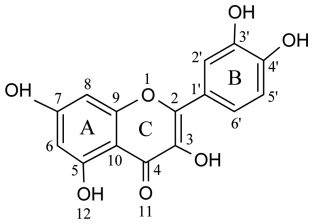

Scheme 1. The molecular structure of quercetin.

Surfactants dissolved in nonpolar solvents assemble to form reverse micelles. In this system, the polar head groups of amphiphiles aggregate to form a micellar core and the hydrophobic tails extend into the bulk solvent. Among all possible micelle systems, aerosol-OT (sodium 1,4-bis[2-ethylhexyl] sulphosuccinate, AOT) in alkanes (*e.g. n*-heptane or isooctane) has been the most widely studied for its ability to form reverse micellar aggregates and for its ability to solubilize and compartmentalize relatively large amounts of water within its central core. The amount of water in AOT/H_2O/alkane reverse micelles is expressed as the molar ratio of H_2O to AOT ($R = [H_2O]/[AOT]$). The hydrodynamic radius of the spherical aqueous micellar core increases gradually as the amount of water in the micelle increases.[20] The water solubilized in a AOT reverse micelle is similar to the interfacial water near biological membranes or at protein surfaces.[21,22] The peculiar behavior of this water has been attributed to its strong interaction with the ionic head groups of the surfactant and counter ions as well as to the overall disruption of the three-dimensional hydrogen bond network usually present in bulk water.[23-26] For this reason, the AOT micelle has been regarded to behave like a membrane mimetic system. As the size of the water pool increases due to the addition of water, the microviscosity of the solubilized water decreases as its polarity increases. As the amount of water increases, the average aggregation number of micelles increases dramatically, regardless of the hydrocarbon solvent used or the AOT concentration.[27] Moreover, this AOT reverse micelle is an excellent solvent system for spectroscopic measurements because AOT/H_2O/alkane systems are homogeneous

†This paper is to commemorate Professor Myung Soo Kim's honourable retirement.

and optically transparent over a wide range of conditions such as temperature, concentration *etc*.

This work is a comprehensive study of the fluorescence properties of QCT in various AOT/H_2O/heptane reverse micelles by steady-state and time-resolved fluorescence spectroscopy. Also, the location of QCT inside a micelle and the structure of the AOT micelle as a function of the amount of water are investigated. Besides providing important information about the mechanism underlying the strong biological activities of such flavonoid, this study will provide more insight into the characteristic properties of AOT reverse micelles.

Experimental

QCT and NaAOT (SigmaUltra) were purchased from Sigm-Aldrich Chemical Co. (St Louis, U.S.A) and used without further purification. A few studies showed that there was no difference between purified AOT preparations and unpurified commercially available compounds.[28] *n*-Heptane (spectrophotometric grade) and methanol (spectrophotometric grade) were also obtained from Sigma-Aldrich and used as received. Deionized, twice-distilled water was used to prepare the stock and sample solutions.

To avoid any oxygen effects, the methanol for preparing the QCT stock solution was deaerated with high purity Ar gas purging for 90 min. The AOT was dried for 48 hours in vacuum at 1×10^{-3} torr with P_2O_5, and kept in a desiccator over P_2O_5. A 3% (wt/vol) AOT/heptane stock solution was used for all experiments. Low concentration solutions (below 1×10^{-5} M) were used to avoid any primary or secondary interfilter effects. The sample preparation method was described in detail in a previously published paper.[18] In the micelle systems, the surfactant/solute ratio was about 1.7×10^4, equivalent to micelle/solute ratios of roughly 740 (R = 0) and 50 (R = 20) for surfactant aggregation numbers of 23 (R = 0) and 333 (R = 20), respectively, which were measured for the AOT/alkane solution.[29,30] Therefore, no more than one solute molecule occupies a given micelle on average, precluding significant aggregation effects. Furthermore, under such conditions, the perturbation of the structure and related properties of the AOT reverse micelles by the solubilization of QCT molecules would be negligible.

The UV/visible absorption spectra were measured using a JASCO V-530 UV/visible spectrophotometer at room temperature. Steady-state fluorescence spectra were obtained using a Perkin-Elmer LS-50B spectrofluorometer. Fluorescence quantum yields were measured using anthracene (Φ = 0.27) as a reference.[31-33] The fluorescence lifetimes and other time domain data were obtained by using the time-correlated single-photon counting method with the Fluorolog-3 spectrofluorometer (HORIBA, Edison, NJ, USA). The sources were fixed wavelength interchangeable NanoLED pulsed laser-diodes and LEDs. The standard optical pulse durations were < 200ps (< 100 ps typical) for laser-diodes and < 1.5 ns for LEDs. Repetition rate was up to 1 MHz and lifetimes were measured from < 100 ps to 100 μs. To remove the dissolved oxygen before the fluorescence measurements, the sample solution were degassed by high purity Ar gas purging for 20 min.

Results and Discussion

To understand the spectroscopic properties of QCT in AOT reverse micelles, it is important to find out the position that this molecule occupies inside the micelle. Two distinct water domains appear in the polar core; bound water and free water in the central region.[26] First, the water added to a micelle hydrates ions and the head groups of surfactant molecule preferentially. After all the ionic species have been fully solvated, the remaining water starts to enter the micelle core as a bulk-like free water. In an AOT/H_2O/heptane system, four distinct solubilizable areas are available: hydrocarbon continuum, AOT interface, bound water interface, and inner free water pool. The properties of each environment change as the amount of water in the micelle increases. QCT is insoluble in n-heptane, slightly soluble in water, and soluble in CH_3OH and CH_3CN. Therefore, QCT does not reside outside the micelles or even in the middle of the alkyl tails of the surfactants. It has been reported that fluoroquinolone antibiotics are closely associated with micelles and reside at the bound water interface near the surfactant headgroups.[26] Since the QCT is similar in solubility and molecular size to fluoroquinolones, it can be concluded that QCT resides at the same place, namely the bound water interface and interacts with this micellar interface strongly, regardless of the amount of water in the micelle.

The UV-visible absorption spectra of QCT in various solvents are presented in Figure 1. The absorption spectra in CH_3OH and CH_3CN are about the same, with two absorption bands around 370 nm (Band I) and 255 nm (Band II). However, the absorption spectra in the AOT micelle are different from with those in organic solvents. In the AOT micelle, the Band II exhibits a large blue shift and Band I shows a small side band around 385 nm. This indicates that although the molecular structure of QCT was not changed significantly by the CH_3OH or CH_3CN solvent, it was somewhat influenced by the AOT micelle system. The UV-visible absorption spectra of QCT in various AOT reverse micelles

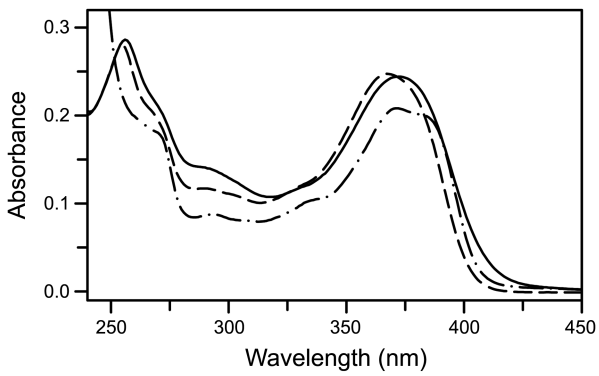

Figure 1. UV/visible absorption spectra of quercetin in various solvents; (1) CH_3OH (———), (2) CH_3CN (– – – –), (3) 3% AOT reverse micelle; R = 0 (–·–·–).

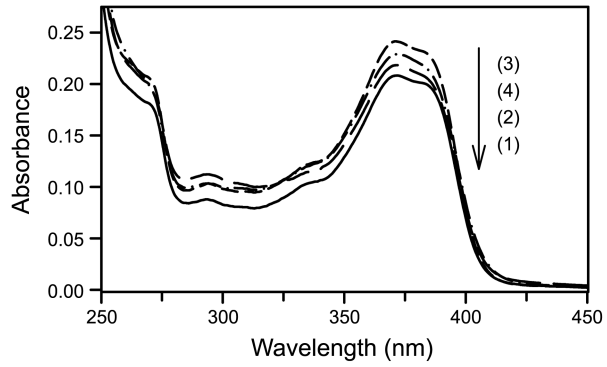

Figure 2. UV/visible absorption spectra of quercetin in various 3% AOT reverse micelles; (1) R = 0 (———), (2) R = 4.0 (– – – –), (3) R = 10.0 (------), (4) R = 20.0 (–·–·–).

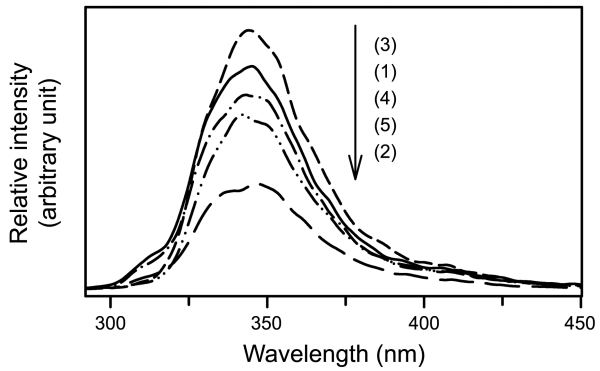

Figure 3. Steady-state fluorescence emission spectra of quercetin in various 3% AOT reverse micelles; (1) R = 0 (———), (2) R = 4.0 (– – – –), (3) R = 10.0 (------), (4) R = 20.0 (–·–·–), (5) R = 30.0 (–··–··–).

are shown in Figure 2. As the R value increases, the shape and band position do not change but the absorbance of Band I changes slightly. The inside of an AOT reverse micelle is heterogeneous. So, if QCT inside the micelle moves to different positions as water is added, the absorption band shape and position would change. Therefore, this fact indicates that the position of the QCT molecule inside AOT micelles does not change due to the QCT molecule's strong interaction with the bound water interface even when the amount of water in the micelle increases.

The QCT with the 5-OH group has been known as a non-fluorescent compound in aqueous solutions.[10-12] However, it gave new fluorescence emission spectra in various hydro-organic mixed solvents when it was excited to the second excited state under 255 nm light, which corresponded to the maximum absorption of Band II. However, when 370 nm radiation, which corresponded to the maximum absorption of Band I, was used as the excitation source, no fluorescence emission was observed in the same mixed solvents.[14,34] Similar fluorescence properties were also exhibited in AOT reverse micelles. As shown in Figure 3, steady-state fluorescence emission spectra were observed around 345 nm when 270 nm radiation was used as the excitation light, but no fluorescence spectra were observed when the 370 nm long-wavelength light was used to excite the molecule. Because the wavelength of this emission band is shorter than the wavelength of the absorption band around 370 nm, the fluorescence spectra in Figure 3 originated from the $S_2 \rightarrow S_o$ transition. The shape and position of the peak did not change significantly due to the addition of water, while the intensity of the peak varied with a regular pattern as a function of water concentration in the micelle, meaning that the position of QCT inside the micelle did not change with the increasing amount of water in the micelle. As a result, the variation of the environment at a distinct area inside the micelle due to the addition of water will change the spectral intensity. As the R value increases from zero to around 7, the emission intensity decreases linearly. Beyond $R \cong 7$, the fluorescence intensity increases sharply and reaches the maximum value at the $R \cong 10$. If the R value increases beyond 10, the fluorescence intensity will decrease almost linearly.

To understand the spectroscopic properties of QCT, it is essential to study its geometrical molecular structure. Especially, the dihedral angle, which defines the position of the B ring with respect to the γ-pyrone ring (A and C rings), is the most important. Since the energy barrier for the rotation of the B ring on the C(2) – C(1') bond is very low, the B ring can rotate easily on this side and the molecule can approach a planar structure.[35,36] Because the hydrogen bond-like interaction will exist between the 3-OH moiety and the proton on C(2') or C(6'), the optimized dihedral angle in the gas phase is close to 0°. Eventually, because the molecular structure is completely planar, QCT is completely conjugated. Also, since the QCT has both an electron donor and acceptor, it will become good donor-acceptor-conjugated molecule.[14,18,34] At the excited state, the initial molecules (N) will become of the charge transferred zwitterionic form (T) induced by the excited state intramolecular charge transfer (ESICT). The T form will be stabilized further owing to the large delocalization of the π electrons throughout the whole molecule. Usually, a fluorescence emission spectrum is roughly the mirror image of the absorption spectrum. However, such mirror image relationship was not observed in QCT. This fact supports further the occurrence of this ESICT because the shapes of absorption and emission spectra will be very different if the geometry and dipole moment change greatly owing to the absorption of light. This ESICT can usually cause a stronger fluorescence emission because the excited state becomes more stable and tolerable for any quenching effect owing to the existence of the resonance forms.

The study of the intramolecular hydrogen bonding is also important for understanding the spectroscopic properties of QCT because this kind of hydrogen bonding is regarded as the most important stability criterion.[34,37] QCT can form two important intramolecular hydrogen bonds between 5-OH and O-11 and between 3-OH and O-11. The intramolecular hydrogen bond between 5-OH and O-11, which forms a stable six-membered ring, is stronger than that between 3-OH and O-11.[10,35,38-40] For this reason, the QCT, 5-hydroxyflavone, has a dramatically different excited state behavior from that of 3-hydroxy flavone, which have only the –OH group at the C-3.[10,11] Excited state intramolecular proton transfer (ESIPT) between 5-OH and O-11 by "keto-enol

tautomerization" has been observed in 5-hydroxyflavone and other many molecules having this kind of intramolecular hydrogen bond.[41-44] Martinez *et al*. reported the direct evidence of ESIPT between 5–OH and O-11 in 5-hydroxyflavone.[13] For QCT, it is reasonable to assume that this ESIPT also occurs *via* the intramolecular hydrogen bond between 5-OH and O-11.[14] However, it is very important that this ESIPT occurs in the S_1 state but seldom appear in the S_2 state.[14,18] Because the pseudo-Jahn-Teller distorted excited state of QCT and other 5-hydroxyflavone will be formed by this ESIPT, these molecules do not exhibit any $S_1 \rightarrow S_o$ fluorescence emission.[10,34,45] Also, it is known that the Franck-Condon (FC) factors involved in the $S_2 \rightarrow S_1$ internal conversion will be very small.[18] Therefore, at the S_2 state, ESIPT can not occur, but ESICT can. Furthermore, the rate of the $S_2 \rightarrow S_1$ internal conversion will be very slow owing to the small FC factor. For these reasons, only the $S_2 \rightarrow S_o$ fluorescence emission will be observed if the QCT is excited to the S_2 state.

The fluorescence properties of QCT corresponding to $S_2 \rightarrow S_o$ emission are shown in Table 1. The method for calculating the radiative (k_r) and nonradiative rate constants (k_{nr}) was explained in a previous paper.[34] The quantum yields decrease gradually as the amount of water in the micelle increases until R = 7.0. As the strength of the intermolecular hydrogen bond between QCT and H_2O increases due to the addition of water in the micelle, the quantum yields decrease.[14,34] When R = 10.0, the quantum yield shows the maximum value. As the R value increases beyond 15.0, the quantum yield does not exhibit any significant changes. When water is added to the micelle first, the bound water interface environment will change greatly because the added water solvates counter cations and the head groups of the surfactant molecules in this area preferentially. So, if the R value is smaller than 10, the bound water increases with no free water actually owing to the addition of water in the micelle. As the R value become greater than 15, free water will begin to appear. When the R value is around 15, the number of bound water per surfactant molecule reaches roughly the maximum value. Beyond this R value, since the number of free water will begin to increase sharply, the bound water interface environment will not change significantly as the increase of water concentration in micelle.[26] In the case of a large R value (R > 15), if QCT resides at the well-defined free water pool in the micelle core, the quantum yield should decrease with increasing water concentration. Therefore, this change of fluorescence quantum yield as a function of R value strongly supports the fact that QCT resides at the bound water interface, not in the well-defined inner free water pool, and interacts strongly with the sodium ions, waters and polar groups of the surfactant regardless of the amount of water in the micelle. The change of fluorescence lifetime as a function of the R value also exhibits a similar pattern as that of the quantum yields. Until R = 10.0, the lifetime decreases gradually as the amount of water in the micelle increases. If the R value is larger than 10, the lifetime decreases rapidly. Therefore, the quantum yield and lifetime change greatly around R = 10-15.

Table 1. The fluorescence quantum yields (Φ), fluorescence lifetimes (τ), and radiative (k_r) and nonradiative rate constants (k_{nr}) of quercetin in AOT reverse micelle. λ_{ex} = 270 nm

R[a]	Φ (10^{-3})[b]	τ (ns)[c]	k_r (10^6 s^{-1})	k_{nr} (10^8 s^{-1})
0.0	13.5	5.67	2.38	1.74
2.0	9.26	4.87	1.90	2.03
4.0	7.51	3.28	2.29	3.03
7.0	6.59	3.29	2.00	3.02
10.0	14.8	2.95	5.02	3.34
15.0	11.0	1.90	5.79	5.21
20.0	10.6	1.87	5.67	5.29
30.0	10.8	2.57	4.20	3.85

[a]The molar ratio of water to AOT. [b,c]Uncertainty ≤ 10%

To more closely study the influence of water concentration on the fluorescence properties of QCT in the AOT micelle, the logarithms of the radiative and nonradiative rate constants were plotted as a function of R value, as shown in Figure 4. When R value is smaller than 10, the ln(k_r) is small and approximately constant, but if the R value exceeds 10, ln(k_r) increases sharply and does not show any significant change due to the increase of the R value in the micelle. This fact support further that the bound water interface environment does not change greatly with increasing amount of water in the micelle if the R value is larger than 10, and that the QCT resides at the bound water interface regardless of the water concentration in the micelle. In the ln(k_{nr}) *vs* R plot, ln(k_{nr}) increases rapidly with the addition of water in the micelle until R ≅ 15. As the R value is larger than 15, ln(k_{nr}) is roughly constant and rather decreases. These results are approximately consistent with the changes of the quantum yield and lifetime as a function of water concentration in the micelle. Therefore, following two facts can be reconfirmed by examining these ln(k_r) *vs* R and ln(k_{nr}) *vs* R plot: first, the environment around the bound water interface near the ionic and polar surfactant head group changes greatly with the addition of water in the micelle until R = 10-15 but the properties of this interface are nearly unchangeable at R > 10-15 because of the appearance of the free water from this point; second, QCT inside the AOT micelle is located at the bound water interface. This position of the QCT in the micelle does not change significantly as the R value increases.

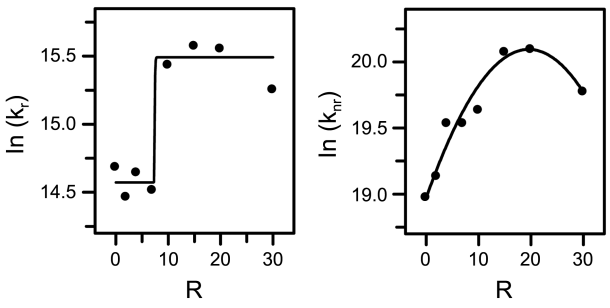

Figure 4. Logarithms of the radiative rate constants, k_r and nonradiative rate constants, k_{nr}, plotted as a function of the molar ratio of water to AOT, R, in the 3% AOT reverse micelle. The solid lines are the best polynominal regression fit to the data.

Conclusion

The UV-visible absorption spectra of QCT in the AOT micelle are somewhat different from those in CH_3OH and CH_3CN. As the water concentration in the micelle increases, the shape and band position of the absorption spectra do not change but the absorbance of Band I changes slightly. Since the QCT has both an electron donor and acceptor, and its molecular structure is completely planar, the ESICT can occur at the excited state. Although this ESICT can usually result in strong fluorescence emissions, QCT is known as a nonfluorescent molecule owing to the formation of the distorted excited state by ESIPT. This ESIPT can occur *via* the intramolecular hydrogen bond between 5-OH and O-11. Since this ESIPT will occur at the S_1 state, $S_1 \rightarrow S_o$ fluorescence emission is totally absent. However, since ESIPT cannot occur at the S_2 state and FC factors involved in the $S_2 \rightarrow S_1$ internal conversion will be very small, $S_2 \rightarrow S_o$ fluorescence emission can be observed if the QCT is excited to the S_2 state. As the amount of water in the micelle increases, the fluorescence intensity changes in a regular pattern without any change of band shape and position.

The changes of fluorescence quantum yields and lifetimes were measured as a function of water concentration in the AOT micelle. Also, the radiative and nonradiative rate constants were calculated at various R values. Using all of these results, the following facts can be confirmed. Because the first added water will hydrate ions and polar group of surfactant preferentially and the first free water will begin to appear at the $R \cong 15$, the physical properties around the bound water interface change greatly due to the increase of water concentration until R = 10-15. Also, QCT resides at the bound water interface and the position of QCT inside the micelle does not change significantly due to the strong interaction of QCT with the micellar interface regardless of the amount of water in the micelle.

Acknowledgments. This research was supported by the Basic Science Research Program through the National Research Foundation of Korea (NRF) funded by the Ministry of Education, Science and Technology (2010-0023938). Also, this work was supported by the Gyeongsang National University Fund for Professors on Sabbatical Leave, 2012.

References

1. Bondarev, S. L.; Knyukshto, V. N. J. *J. Luminescence* **2013**, *142*, 236.
2. Gradisar, H.; Pristovsek, P.; Plaper, A.; Jerala, R. *J. Med. Chem.* **2007**, *50*, 264.
3. Katiyar, S.; Elmets, C. A.; Katiyar, S. K. *J. Nutrit. Biochem.* **2007**, *18*, 287.
4. Caturla, N.; Vera-Samper, E.; Villalain, J.; Mateo, C. R.; Micol, V. *Free Radical Biol. Med.* **2003**, *34*(6), 648.
5. Yang, C. S.; Chung, J. Y.; Yang, G.; Chhabra, S. K.; Lee, M. J. *J. Nutr.* **2000**, *130*, 472.
6. Rothwell, J. A.; Day, A. J.; Frankel, E. N. J.; Morgan, M. R. A. *J. Agric. Food Chem.* **2005**, *53*, 4355.
7. Schilcher, H.; Patz, B.; Schimmel, K. C. H. *Aerctezeitschrift fuer Naturheilverfahren* **1990**, *31*, 819.
8. Gaberscik, A.; Voncina, M.; Trost, T.; Germ, M.; Bjoern, L. O. *J. Photochem. Photobiol. B: Biol.* **2002**, *66*, 30.
9. Heim, K. E.; Tagliaferro, A. R.; Bobilya, D. J. *J. Nutrit. Biochem.* **2002**, *13*, 572.
10. Falkovskaia, E.; Sengupta, P. K.; Kasha, M. *Chem. Phys. Lett.* **1998**, *297*, 109.
11. Sengupta, P. K.; Kasha, M. *Chem. Phys. Lett.* **1979**, *68*, 382.
12. Smith, G. J.; Markham, K. R. *J. Photochem. Photobiol. A* **1998**, *118*, 99.
13. Martinez, M. L.; Studer, S. L.; Chou, P. T. *J. Am. Chem. Soc.* **1991**, *113*, 5881.
14. Park, H. R.; Daun, Y.; Park, J. K.; Bark, K. M. *Bull. Korean Chem. Soc.* **2013**, *34*, 211.
15. Bilski, P. L.; Martinez, J.; Koker, E. B.; Chignell, C. F. *Photochem. Photobiol.* **1998**, *68*, 20.
16. Park, H. R.; Oh, C. H.; Lee, H. C.; Lee, J. K.; Yang, K.; Bark, K. M. *Photochem. Photobiol.* **2002**, *75*, 237.
17. Liu, W.; Guo, R. *Colloids Surf. A* **2006**, *274*, 192.
18. Park, H. R.; Liu, H. B.; Shin, S. C.; Park, J. K.; Bark, K. M. *Bull. Korean Chem. Soc.* **2011**, *32*, 981.
19. Liu, W.; Guo, R. *J. Coll. Inter. Sci.* **2006**, *302*, 625.
20. Fletcher, P. D. I.; Howe, A. M.; Robinson, B. H. *J. Chem. Soc. Faraday Trans. I* **1987**, *83*, 985.
21. Grigolini, P.; Maestro, M. *Chem. Phys. Lett.* **1986**, *127*, 248.
22. D'Aprano, A.; Lizzio, A.; Turco Liveri, V.; Aliotta, F.; Vasi, C.; Migliardo, P. *J. Phys. Chem.* **1988**, *92*, 4436.
23. Jain, T. K.; Varshney, M.; Maitra, A. *J. Phys. Chem.* **1989**, *93*, 7409.
24. Riter, R. E.; Undiks, E. P.; Levinger, N. E. *J. Am. Chem. Soc.* **1998**, *120*, 6062.
25. Riter, R. E.; Willard, D. M.; Levinger, N. E. *J. Phys. Chem.* **1998**, *102*, 2705.
26. Park, H. R.; Lee, H. C.; Kim, T. H.; Lee, J. K.; Yang, K.; Bark, K. M. *Photochem. Photobiol.* **2000**, *71*, 281.
27. Fendler, J. H. *Membrane Mimetic Chemistry: Characterization and Applications of Micelles. Microemulsions, Monolayers, Bilayers, Vesicles, Host-Guest Systems, and Polyions, Chapter 3*; John Wiley & Sons: New York, USA, 1982; p 652.
28. Politi, M. J.; Brandt, O.; Fendler, J. H. *J. Phys. Chem.* **1985**, *89*, 2345.
29. Wong, M.; Thomas, J. K.; Nowak, T. *J. Am. Chem. Soc.* **1977**, *99*, 4730.
30. Paulo, P. M. R.; Laia, C. A. T.; Costa, S. M. B. *J. Phys. Chem. B* **2003**, *107*, 1097.
31. Bark, K. M.; Forcé, R. K. *Spectrochim. Acta* **1993**, *49A*, 1605.
32. Eaton, D. F. *Reference Compounds for Fluorescence Measurement*; IUPAC Organic Chem. Division: Wilmington, Delawere, USA, 1987; pp 1-11.
33. Demas, J. N.; Grosby, G. A. *J. Phys. Chem.* **1971**, *75*, 2463.
34. Liu, H. B.; Daun, Y.; Shin, S. C.; Park, H. R.; Park, J. K.; Bark, K. M. *Photochem. Photobiol.* **2009**, *85*, 934.
35. Cornard, J. P.; Merlin, J. C.; Boudet, A. C.; Vrielynck, L. *Biospectros.* **1997**, *3*, 183.
36. Marković, Z.; Milenković, D.; Đorović, J.; Marković, J. M. D.; Stepanić, V.; Lučić B.; Amić, D. *Food Chem.* **2012**, *134*, 1754.
37. Cornard, J. P.; Boudet, A. C.; Merlin, J. C. *J. Mol. Struct.* **1999**, *508*, 37.
38. Mendoza-Wilson, A. M.; Glossman-Mitnik, D. *J. Mol. Struct. (Theochem)* **2004**, *681*, 71.
39. Rossi, M.; Rickles, L. F.; Halpin, W. A. *Bioorg. Chem.* **1986**, *14*, 55.
40. Park, H. R.; Chung, K. Y.; Lee, H. C.; Lee, J. K.; Bark, K. M. *Bull. Korean Chem. Soc.* **2000**, *21*, 849.
41. Bisht, P. B.; Petek, H.; Yoshihara, K.; Nagashima, U. *J. Chem. Phys.* **1995**, *103*, 5290.
42. Sobolewski, A. L.; Domcke, W. *Chem Phys.* **1994**, *184*, 115.
43. Herek, J. L.; Pedersen, S.; Bañares, L.; Zewail, A. H. *J. Chem. Phys*. **1992**, *97*, 9046.
44. Zhu, A.; Wang, B.; White, J. O.; Drickamer, H. G. *J. Phys. Chem. B* **2004**, *108*, 895.
45. Hochstrasser, R. M.; Marzzacco, C. *J. Chem. Phys.* **1968**, *49*, 971.